

MEASUREMENTS OF STRESS EVOLUTION DURING THIN FILM DEPOSITION

E. CHASON AND J.A. FLORO

Sandia National Laboratories, Albuquerque, NM 87185-1415

ABSTRACT

MAY 17 1983

OCTI

We have developed a technique for measuring thin film stress during growth by monitoring the wafer curvature. By measuring the deflection of multiple parallel laser beams with a CCD detector, the sensitivity to vibration is reduced and a radius of curvature limit of 4 km has been obtained *in situ*. This technique also enables us to obtain a 2-dimensional profile of the surface curvature from the simultaneous reflection of a rectangular array of beams. Results from the growth of SiGe alloy films are presented to demonstrate the unique information that can be obtained during growth.

INTRODUCTION

Understanding and controlling stress in thin films is critical for tailoring their optical, electronic and mechanical properties. Precise control of layer strain is required for the production of compound semiconductor heterostructure devices, and stress induced process can lead to the failure of interconnects and delamination of films. In general, most studies of thin film stress are performed after the films are grown. In this work, we discuss a new approach for measuring stress evolution *in situ* during the growth of thin films. We present results from experiments during epitaxial growth of SiGe alloy layers on Si(001) substrates with particular emphasis on the new information about the growth process that can be obtained from real time stress measurements.

WAFER CURVATURE MEASUREMENTS USING LASER BEAMS

A thin film under stress on a substrate will lead to bending of the substrate [1]. The radius of curvature of the substrate that results will be due to the balancing of the external bending moment applied and the bending moment of the curved substrate. The resulting curvature can be detected by the deflection of a beam of light incident upon the sample. If the substrate is flat, then the angle of reflection will be the same anywhere on the surface. However if the substrate is curved, then the reflection angle will change as the beam is move across the surface.

Various experimental approaches have been devised to measure the curvature of the surface. The scanning mirror technique [2,3,4,5] uses a rotating mirror and lens to scan the laser beam across the sample without changing the angle of incidence. A position sensitive detector measures the deflection of the beam as it is scanned. Alternatively, a beam splitter has been used [6,7,8] to produce two parallel beams whose deflections are measured independently with position sensitive detectors.

We have developed a variation of this technique with some features that simplify its use as an *in situ* diagnostic during growth. The experimental setup is shown in figure 1. An etalon that has been coated with highly reflective layers on both sides is placed at an angle to the laser beam. The non-normal incidence leads to multiple internal reflections inside the etalon so that a linear array of parallel beams is formed. The high degree of parallelism of the etalon faces ensures that the exiting beams are all parallel. These multiple parallel beams are then reflected simultaneously from the sample surface and measured with a CCD camera. The objective lens is used to focus

MASTER
DISTRIBUTION OF THIS DOCUMENT IS UNLIMITED
DUC



the beams directly onto the CCD array so that no camera lens is necessary. Typically, five beams can be imaged on the CCD array simultaneously.

The use of multiple beams has several beneficial features for *in situ* measurement. First of all, the optics are very simple. The spatial filter and objective lens can be aligned before mounting on the deposition system and generally require only minimal subsequent alignment. Because a CCD camera is used, the reflected spots are fully imaged and can be viewed on a television monitor for focusing of the objective lens. In addition, because the CCD array has a relatively large active area, if the spots move due to sample motion (for instance during heating) this does not generally require realignment of the camera.

Simultaneous measurement of the multiple spots and no beam scanning make the system inherently less sensitive to sample vibration than the scanning mirror technique. Since all the laser spots move together, noise due to position changes or tilt of the sample do not appear as changes in the curvature. A quantitative representation of this is shown in figure 2. The sample in this run was unconstrained (held by gravity) and would sometimes exhibit a rocking motion, possibly driven by vibrations in the vacuum pumps used on the MBE system. In figure 2a, the variation in time of one of the spot centroids is shown; the excursions correspond to an RMS noise of 4.3 pixels. However the variation in time of the difference between the centroid of this spot and the spot adjacent to it (separated by approximately 120 pixels) is much smaller. Shown in figure 2b, the spacing between the centroids has an RMS deviation of only 0.09 pixels. So even though the positions of the spots may not be stable, the difference between the spots is much less sensitive to vibration.

2-DIMENSIONAL CURVATURE PROFILES

From the relative deflection of adjacent beams, we are able to determine the profile of the curvature across the sample. This is an advantage over the measurements using a beam splitter where only a single beam spacing is obtained. By using a pair of reflective optics oriented orthogonally to the laser beam, we are able to produce a two-dimensional grid of spots on the sample to obtain a two-dimensional curvature profile simultaneously. The results of this technique are shown in figure 3. The sample configuration is shown in figure 3a; the sample is clamped at one end in a cantilever arrangement. The spots are incident on the sample at the positions shown in the figure. The reflected spot positions are shown in figure 3b for the as-prepared sample (o) and the sample after growth of 72 angstroms of Si₆₅Ge₃₅ (+). The centroids of the two beam profiles have been made to coincide to remove the effect of tilting of the sample. The difference between the spot positions of the flat sample and the curved sample can be related to the surface normal of the sample at the point of impact of the beam. From the surface normals, we can reconstruct a map of how the surface has deformed. In figure 3c, we show an image of the surface after the SiGe alloy growth. Note that the curvature is significantly larger along the unconstrained x-axis than along the y-axis where the clamp prevented the wafer from curving. Also note the difference in scales of the z-axis relative to the in-plane x- and y-axis. The maximum vertical deflection of the surface is less than 0.3 microns.

IN SITU MEASUREMENTS OF STRESS EVOLUTION

We have used the *in situ* wafer curvature technique for measuring the evolution of stress during growth of Si_xGe_{1-x} alloys on Si(001) substrates. An example of the stress measurement is shown in figure 4 where the evolution of the product of film stress (σ) and thickness (h) during

growth is demonstrated. The three distinct regions of behavior observed during growth are discussed below.

Stress Offset

In the early stages of growth (figure 4a, 0 - 10 Å), the stress increases much more slowly than expected for a strained epitaxial film. We attribute this behavior to segregation of the Ge to the surface during the early stages of growth. After a Ge rich surface layer is formed, the film grows at the nominal composition determined by the growth fluxes. The Ge-rich layer remains on the surface during subsequent growth, presumably by exchanging places with adatoms arriving from the deposition flux. This interpretation is supported by earlier work [9,10] and is also consistent with our measurements of the offset dependence on alloy composition. For decreasing Ge fraction in the film, the offset before the linear elastic regime begins increases since it takes longer to form a surface layer. We also find that growing pure Si after the growth of a SiGe layer results in increasing compressive stress as the surface Ge is re-incorporated into the Si layer. Without the presence of Ge on the surface, the growth of Si would not lead to additional strain since the films are fully pseudomorphic.

Two other possible explanations for this behavior, interface stress and surface morphology, have also been considered. Although interfacial stress can contribute to wafer curvature, it is probably not the dominant source of the offset in figure 4a since the offset is much longer than the time it takes to deposit one monolayer. Alternatively, if the surface is being covered with small islands, it is possible for the islands to be partially strain relaxed without being dislocated. However, simultaneous RHEED (reflection high energy electron diffraction) measurements of the surface morphology during growth indicate that the surface does not develop sufficient roughness to enable significant relaxation by this mechanism.

Linear Elastic Regime

After the initial offset, σh increases linearly with the film thickness. For thicknesses below the limit for introduction of dislocations, the rate of change of σh is equal to $M(\epsilon)\epsilon dh/dt$ where ϵ is the film strain, $M(\epsilon)$ is the biaxial modulus of the strained alloy film and dh/dt is the growth rate. We have measured $d(\sigma h)/dt$ for different alloy compositions to determine the dependence of $M(\epsilon)$ on strain. The growth rates and compositions were calibrated using Rutherford backscattering spectrometry (RBS), double crystal X-ray diffraction and X-ray reflectivity. We find that the biaxial modulus can be explained by a simple rule of mixtures over the range of 15 - 60% Ge concentration where the endpoints are the bulk unstrained elastic constants for Si and Ge [11].

Strain Relaxation

As epitaxial films become thicker during growth, they reach a critical thickness beyond which dislocations can form to decrease the coherency strain energy. The onset of strain relaxation is seen in figure 4b as a decrease in the slope of σh vs. thickness at approximately 400 Å. We have measured the onset of strain relaxation in Si₇₁Ge₂₉ alloys grown at temperatures of 450, 550 and 650 °C [12]. Since the formation of dislocations is thermally activated, the metastable region before the onset of relaxation is larger at lower temperatures. Although strain relaxation kinetics in SiGe alloys have been extensively studied, the laser curvature technique



enables the onset of relaxation and the subsequent kinetics to be measured much more easily than the ex situ techniques that have been previously used.

ACKNOWLEDGEMENTS

We thank Mike Sinclair, Carl Seager and R.C. Cammarata for useful discussions. This work was performed at Sandia National Laboratories and supported by the U.S. Dept. of Energy under contract DE-AC04-94AL85000.

REFERENCES

1. M.F. Doerner, W.D. Nix, CRC Crit. Rev. in Solid State and Mater. Sci. **14**, 225 (1988).
2. P. Flinn, Gardner and Nix. IEEE Trans. Elec. Dev. **ED-34**, 689 (1987).
3. C.A. Volkert, J. Appl. Phys. **70**, 3521 (1991).
4. J.A. Ruud, A. Witvrouw and F.A. Spaepen, J. Appl. Phys **74**, 2517 (1993).
5. A.L. Shull, H.G. Zolla and F.A. Spaepen, Mat. Res. Soc. Symp. Proc. **356**, 345 (1995).
6. R. Martinez, A. Augustyniak and J.A. Golovcenko, Phys. Rev. Lett. **64**, 1035 (1990).
7. A. Schell-Sorokin and R. Tromp, Phys. Rev. Lett. **64**, 1039 (1990).
8. Geisz et al., J. Appl. Phys. **75**, 1530 (1994)
9. K. Fujita, S. Fukutsu, H. Yaguchi, Y. Shiraki and R. Ito, Appl. Phys. Lett. **59**, 2103 (1991).
10. D.J. Godbey and M.G. Ancona, Appl. Phys. Lett. **61**, 2217 (1992).
11. J.A. Floro and E. Chason, unpublished.
12. J.A. Floro and E. Chason, Mat. Res. Soc. Symp. Proc. 1996 (in press).

DISCLAIMER

This report was prepared as an account of work sponsored by an agency of the United States Government. Neither the United States Government nor any agency thereof, nor any of their employees, makes any warranty, express or implied, or assumes any legal liability or responsibility for the accuracy, completeness, or usefulness of any information, apparatus, product, or process disclosed, or represents that its use would not infringe privately owned rights. Reference herein to any specific commercial product, process, or service by trade name, trademark, manufacturer, or otherwise does not necessarily constitute or imply its endorsement, recommendation, or favoring by the United States Government or any agency thereof. The views and opinions of authors expressed herein do not necessarily state or reflect those of the United States Government or any agency thereof.

FIGURE CAPTIONS

Figure 1. Schematic of system for measurement of wafer curvature using multiple parallel beams.

Figure 2. (a) Measurement of the positional variation in the centroid of one of the beams reflected from the sample. The RMS noise corresponds to 4.3 pixels. (b) Measurement of the variation in the difference between the centroids of adjacent beams reflected from the sample. The RMS noise (0.09 pixels) is reduced by a factor of 40 from the noise in the centroid positions.

Figure 3. Reflection of a 2-dimensional array of parallel beams from the sample provides a 2-dimensional profile of the surface curvature. (a) Schematic of the sample configuration with one end clamped showing where the laser beams intersect the sample. (b) Position of the centroids of the reflected beams for the as-prepared sample (o) and after the growth of 72 Å of a Si₆₅Ge₃₅ strained film (+). (c) Profile of the curved sample surface after alloy growth reconstructed from the measured change in the surface normal.

Figure 4. Evolution of σ_h during the growth of a Si₇₁Ge₂₉ alloy shows three distinct regions: initial stress offset, linear elastic and strain relaxation. (a) Early stage growth (0-10 Å) shows an initial period of essentially stress-free growth before the linear increase due to coherency strain. (b) Strain relaxation occurs above the critical thickness for dislocation formation.



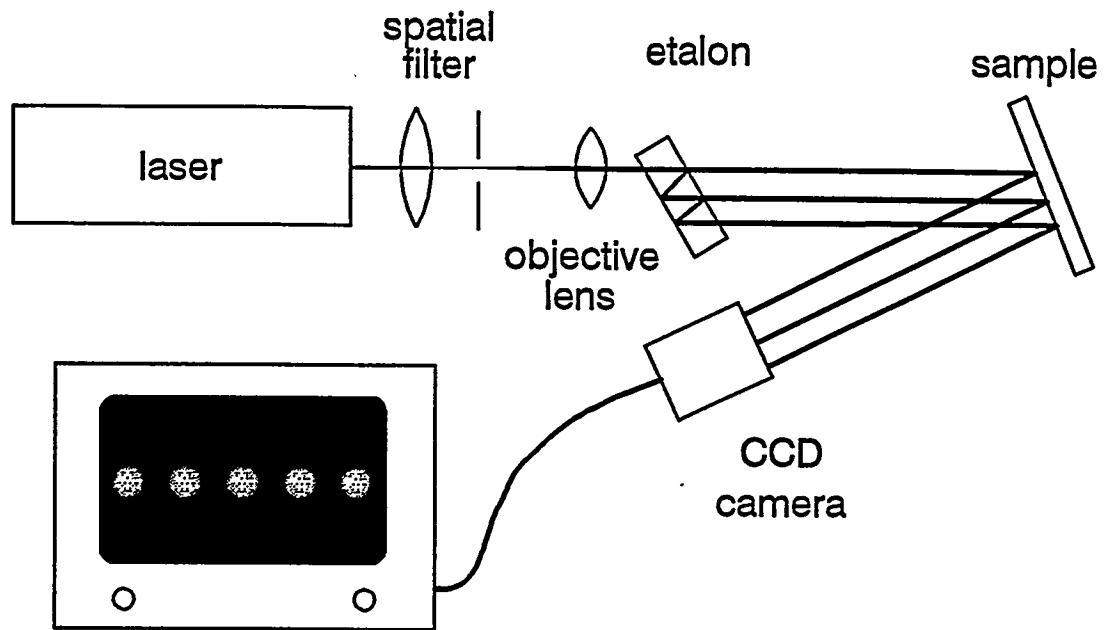


Figure 1.

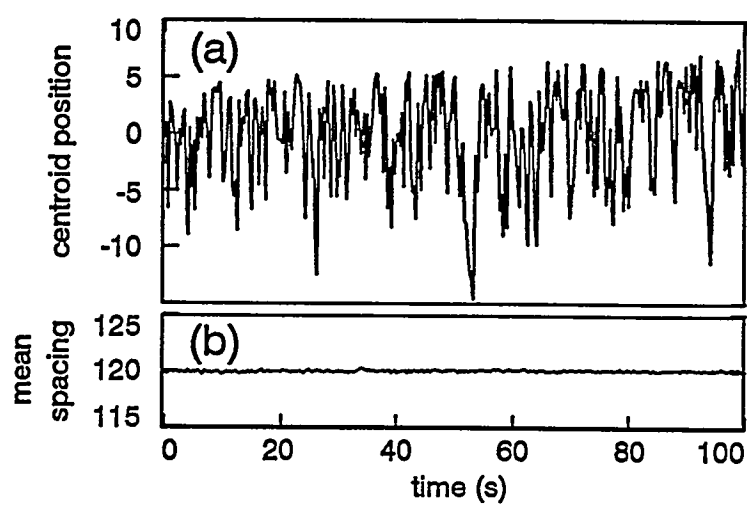


Figure 2.



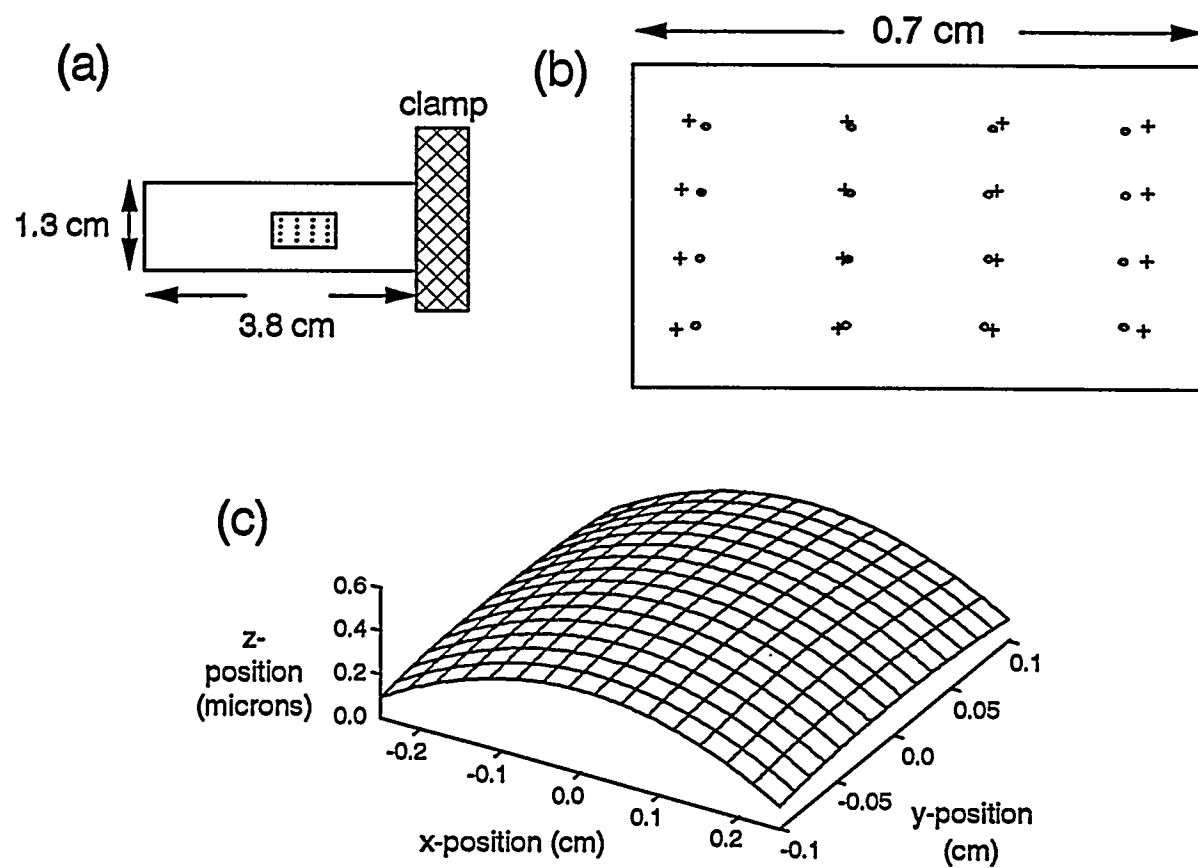


Figure 3

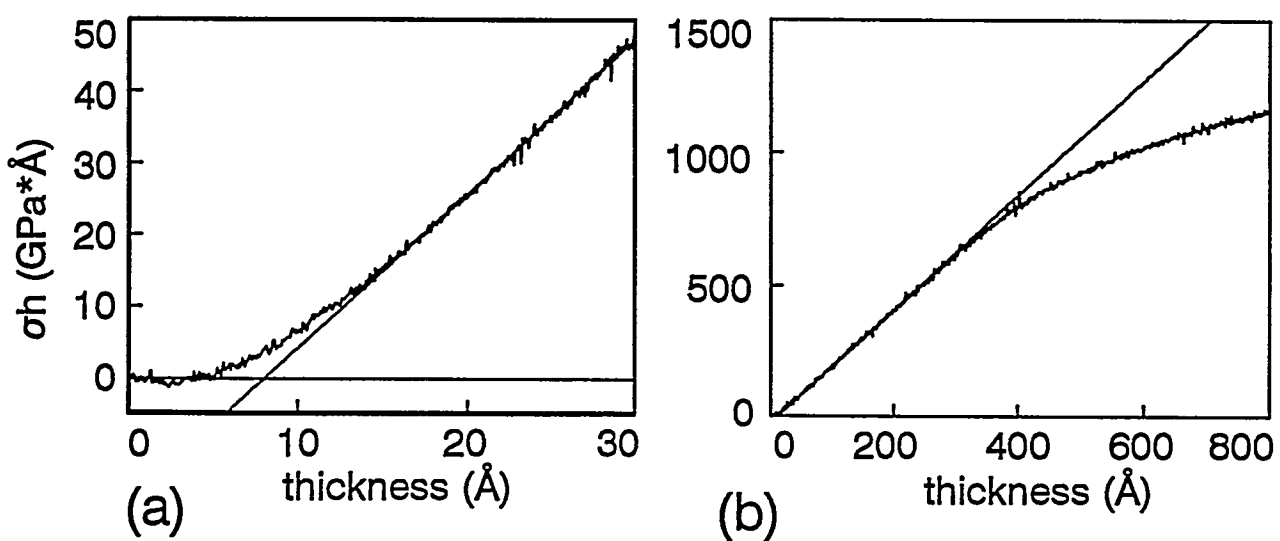


Figure 4

